Experimental Investigation on the Aerodynamic Performance of NLF-0414 Iced-Airfoil

A. Ebrahimi[†], M. Hajipour and H. Hasheminasab

Department of Aerospace Engineering, Sharif University of Technology, Tehran, Iran

†*Corresponding Author Email: ebrahimi_a@sharif.edu*

ABSTRACT

Icing phenomenon on a natural laminar flow airfoil (NLF-0414) has been experimentally investigated. Double horn glaze ice geometry which was acquired during a 15 minutes spray time at $-2.23℃$ with liquid water content and a median volumetric diameter of 1.0 g/m^3 and 20 μm, has been extracted from database of NASA Lewis Research Center. Pressure distribution over airfoil surfacewas evaluated at angles of attack between -2 to 6 degreesfor both iced and clean airfoils. Aerodynamics performance degradation of the iced airfoil has been studied and it is shown that double horn ice accretion, due to its unique geometry, severely affects aerodynamic characteristics of natural laminar flow airfoils. Reattachment locations have been evaluated for upper and lower separation bubbles. The upper surface separation bubble was seen to increase in size in contrary to the lower surface separation bubble.

NOMENCLATURE

Cp	pressure coefficient		x	streamwise coordinate
c	chord			
P	mean static pressure		α	angle of attack
P_∞	free-stream static pressure		ρ	air density
V_∞	free-stream velocity			

1. INTRODUCTION

In a great number of regions, the best locations for the installation of wind turbine stations are along coastal areas or on the tops of hills and mountains. Cold regions are characterized by a potential of wind power 10% higher than other regions, because of their higher air density. Since cold air is denser than warm air, it increases the kinetic energy of wind which leads to further power production of wind turbine (Fortin *et al.* 2005). These locations, however, are inherently susceptible to atmospheric icing events during the cold months of the year. Performance degradation of horizontal axis wind turbines (HAWTs) due to ice accretion has been investigated on a number of machines at different locations (Bose 1992;Pryor 2010;Barber *et al.,* 2011; Han *et al.,* 2012; Homola *et al.,* 2012; Lamraoui *et al.,* 2014; Li *et al.,* 2014).

In addition to the decreased power production, icing causes risk of ice throw and increases dynamic loading of a wind turbine which might lead to a premature failure of turbine components. Ice-mounted blades of a wind turbine also increase noise levels of turbines. Wind turbine can also stop rotating due to heavy vibrations under uneven ice cover (Hochart *et al.,* 2007; Han *et al.,* 2012).

Depending on the icing conditions, ice accretion is categorized into two groups: glaze and rime ice. But most of the time, during an icing event, the ice accreted on the object is heterogeneous, i.e. composed of rime and glaze ice (Fortin and Perron 2009). Usually rime ice is associated with colder temperatures (below $-10℃$), lower liquid water contents and smaller median volumetric diameters which force all the water collected in the impingement area tofreeze on impact. Often, rim ice takes on the original contour of the impingement area which is small and close to the leading edge. Glaze ice is associated with warmer temperatures (above $-10℃$), higher liquid water contents and greater median volumetric diameters which cause only a fraction of the collected waterto freeze in the impingement area and the remaining water runs back and can freeze outside the impingement area (Fortin and Perron 2009). Generally, glaze ice

introduces a more severe drag penalty than rime ice, since it creates an irregular airfoil surface and often has two protruded horns that considerably decrease the lift-to-drag ratio (Han *et al.*, 2012).

Investigations into the accretion of ice and the resulting aerodynamic penalties began as early as the 1940s. Bragg *et al.* (2005) reviewed past research on ice accretion flow field physics and airfoils in icing. In addition to reviewing the flow field of iced airfoils, they proposed an ice shape classification system that was based on the unique flow field features generated by the ice. The proposed classifications are: ice roughness, horn ice, stream wise ice and spanwise-ridge ice. Spanwise-ridge ice is the most dangerous type of ice which usually accretes when there is a heated leading edge ice protected surface. In the absence of ice protecting system, horn ice can be the most dangerous type. Horn ice is usually produced in glaze ice conditions with feather formations downstream of the horns. On iced airfoil, boundary layer separates near the top of the horn and forms a separation bubble. The separation bubble is the dominant flow feature that determines the aerodynamics of an airfoil with a horn ice shape and has a global effect on the airfoil pressure distribution (Bragg *et al.*, 2005).

most past researches about wind turbine icing were focused on the blade icing problem. Bose (1992) researched the icing problem on blade icing of a small-scale HAWT. Homola *et al.*(2010) studied the dependence of atmospheric icing on temperature and wind turbine size by performing numerical simulations of ice accumulation on five different wind turbine blade profiles at four different temperatures. Homola *et al.* (2012) also carried out a numerical study of power performance losses due to ice accretion on a large horizontal axis wind turbine using computational fluid dynamics (CFD) and blade element momentum (BEM) calculations for rime ice conditions.

Li *et al.* (2014) experimentally investigated the characteristics of surface icing on the wind turbine blades with the NACA7715 airfoil. The icing distribution of the blade under different wind speeds and attack angles were obtained by camera. Furthermore, the icing rate and icing area of blade were also calculated and analyzed. Li *et al.* (2010, 2011, 2012) also performed some wind tunnel tests and numerical simulations on the blade icing both for HAWT and VAWT.

The effects of atmospheric icing on the loads and structural responses of a 5-MW land-based wind turbine have been studied by Etemaddar *et al.* (2014). They used computational fluid dynamics code, FLUENT, to estimate the aerodynamic coefficients of the blade after icing. The results were also validated against wind tunnel measurements using a NACA64618 airfoil.

Recently, Jin *et al.* (2015) experimentally studied the effect of a simulated single-horn glaze ice accreted on rotor blades on the vortex structures in the wake of a horizontal axis wind turbine by using the stereoscopic particle image velocimetry (Stereo-PIV) technique.

Roughness and changes in geometry duo to icing phenomenon increase skin friction and pressure drag. One group of airfoils which their aerodynamic performance is very sensitive to ice accretion is NLF series. The natural-laminar-flow (NLF) airfoil was designed in the early 1980s as a medium-speed airfoil with low section drag and high maximum section lift (Colin 1991). Up to now, aerodynamic performance of the airfoil NLF (1)-0414 under different icing conditions has been investigated. Lee and Bragg (1999) performed parametric study to consider the effects of ridge-type ice shape on the performance of a NLF (1)-0414 airfoil. Kim and Bragg (1999) used existing IRT (Icing Research Tunnel)ice-shape data to define a set of glaze ice horn shapes that were tested on a NLF (1)-0414 airfoil. They concluded that the height of the horn had only a small influence on maximum lift when it was located at the airfoil leading edge, perpendicular to the surface, and oriented into the flow. Also Mirzaei *et al.*(2009) investigated unsteady features of flow fields around a glaze-iced NLF (1)-0414.

In the present work, Pressure distribution over a NLF (1)-0414 airfoil with and without simulated glaze ice was experimentally investigated. Unlike most of the parametric researches conducted to date on horn ice which has only considered a single horn, this study focuses on a double horn ice. The simulated ice-shape was based on a leading edge glaze-ice accretion investigated in Lewis Research Center wind tunnel (Colin 1991).

2. EXPERIMENTAL SETUP

The experiments were performed in a low-speed, open-circuit wind tunnel of department of aerospace engineering, K. N. Toosi University of Technology, with a closed wall rectangular test-section of 1.2 m wide, 1 m high, and 3 m long (see Fig. 1). The velocity in the test-section could be continuously varied using an inverter, which controls the rotation speed of the wind tunnel fan. The velocity non-uniformity across the test-section was within ±0.5% and the longitudinal free-stream turbulence intensity was less than 0.2%.

Fig.1. Wind tunnel of department of aerospace engineering, K.N. Toosi University of Technology.

The airfoil model used for this investigation was NLF (1)-0414 with 45 centimeter chord, 75 centimeter span. The simulated ice-shape was based on a leading edge glaze-ice accretion investigated in Lewis Research Center wind tunnel with the geometry shown in Fig. 2. It was acquired during a 15 minutes spray time at −2.23°C with liquid water content and a median volumetric diameter of 1.0 g/m^3 and 20 μm respectively at zero angle of attack. More details about the ice shape may be found in (Colin 1991). A two-dimensional high precision geometrically-scaled foam glaze-ice shape cut by CNC is attached to the leading edge of the model (Fig. 3).

Fig.2. Iced airfoil based on a leading edge glaze-ice accretion investigated in Lewis Research Center wind tunnel

Fig.3. Foam glaze-ice attached on the model.

The surface pressure measurement system was composed of pressure transducers (Honeywell DC005NDC4), a National Instruments A/D board (PCI-6224), Lab VIEW software, F.S.S Pressure Field program and a personal computer. The duration of each pressure record (specified time interval) was 15 s and the sampling rate of 1000 Hz was utilized. In this study, the pressure coefficient C_P, was defined by Eq. (1), where P is the mean static pressure on the surface of the model, P_∞, the free-stream static pressure, V_∞, the free-stream velocity and ρ, the air density. Moreover, the estimated measurement uncertainty of the pressure coefficient was $C_P \pm 0.01$. In order to maintain pressure data, 28 pressure tabs has been used on the model surface. Table 1 shows location of taps.

$$C_P = \frac{P - P_\infty}{0.5\rho V_\infty^2}$$

(1)

Mean pressure distribution data was acquired at Reynolds number of 0.7×10^6 and angles of attack $-2°, 0°, 2°, 4°$ and $6°$. Because of its wet nature, glaze ice shape noticeably deforms with changes in angle of attack (Fortin and Perron 2009). In order to remove ice geometry deformation effects, data

acquisition performed at zero angle of, which the ice has been accreted in, and other small angles of attack. The model was mounted in the test section vertically as Fig. 4 illustrates.

Fig.4. Model in the test section.

Table 1 Locations of pressure taps

Tap	x/c	Tap	x/c	Tap	x/c	Tap	x/c
1	0.02	8	0.26	15	0.86	22	0.33
2	0.06	9	0.33	16	0.03	23	0.39
3	0.10	10	0.40	17	0.06	24	0.46
4	0.12	11	0.49	18	0.11	25	0.53
5	0.15	12	0.60	19	0.15	26	0.65
6	0.17	13	0.70	20	0.21	27	0.75
7	0.20	14	0.78	21	0.27	28	0.82

3. RESULTS AND DISCUSSION

Pressure coefficient distribution over clean and iced airfoils versus normalized streamwise coordinate (x/c), for different angles of attack, is depicted in Figs. 5- 9. At the leading edge of iced airfoil, static pressure is seen to be fairly constant over a particular distance on both upper and lower surfaces. Since in a separation bubble, static pressure is fairly constant(Bragg *et al.,* 2005; Katz 2001), it can be inferred that constant pressure regions at leading edge of the iced airfoil, probably are related to presence of separation bubbles on upper and lower surfaces

Between low momentum fluid trapped in the separation bubble downstream of horn (closer to the wall) and high momentum free stream, a shear layer forms. Similar to separation bubble on a curved surface (Bragg *et al.* 1992), pressure recovery

becomes possible as the shear layer entrains high energy external flow and the bubble reattaches (Fig. 10).
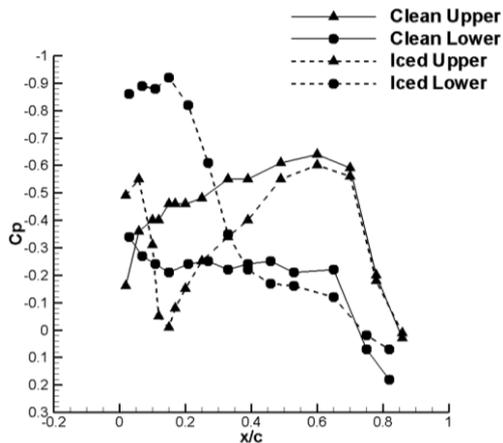
Fig. 5. Pressure distribution over clean and iced airfoils; $\alpha = -2°$.
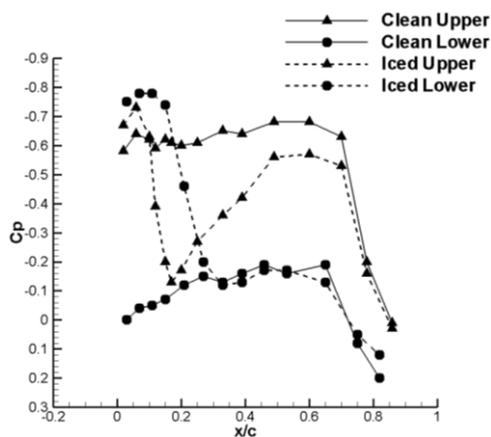
Fig. 6. Pressure distribution over clean and iced airfoils; $\alpha = 0°$.
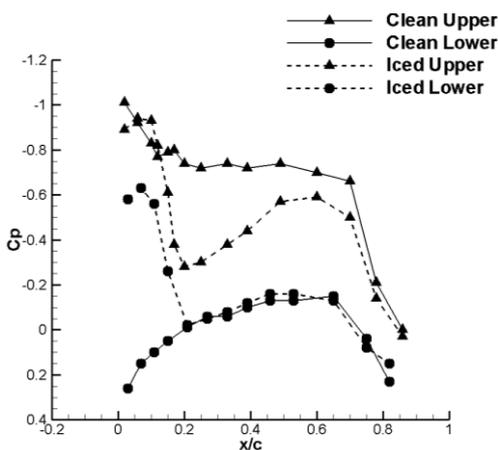
Fig. 7. Pressure distribution over clean and iced airfoils; $\alpha = 2°$.

The reattachment location occurred near the location where the clean and iced pressure distributions intersect on the upper and lower surface. This method of approximating the bubble reattachment location as the intersection of the

clean and iced pressure distributions was investigated by Bragg *et al.*(1992) and was found to be accurate enough. In present study, this method was employed for estimating reattachment point of separated shear layer, downstream of the horn. Dimensionless locations of reattachment points against different angles of attack for upper and lower separation bubbles are presented in Table 2. As might be expected, the upper surface separation bubble was seen to increase in size as the angle of attack was increased, in contrary to the lower surface separation bubble.
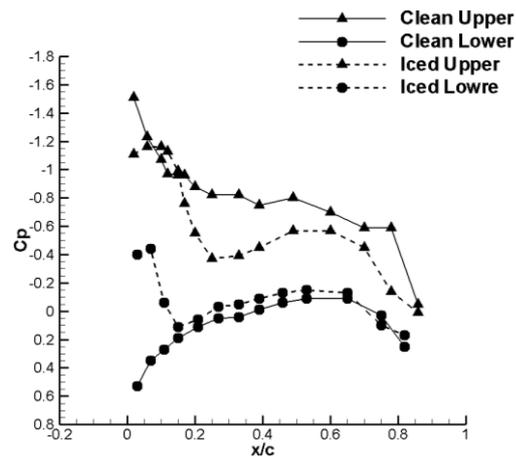
Fig. 8. Pressure distribution over clean and iced airfoils; $\alpha = 4°$.
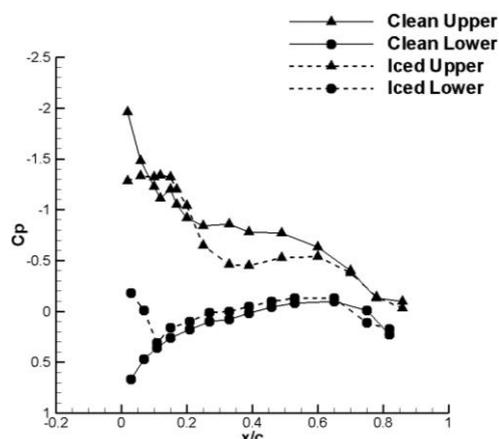
Fig. 9. Pressure distribution over clean and iced airfoils; $\alpha = 6.°$

Table 2 Locations of reattachment points of upper and lower separation bubbles

α (degree)	-2	0	2	4	6
x/c (upper)	0.08	0.1	0.12	0.15	0.22
x/c (lower)	0.39	0.32	0.2	0.15	0.1

In all the experiments, pressure distribution on iced airfoil shows large deviation from clean airfoil, owing to the large extent of separated flow. Aerodynamic characteristics of iced airfoil are affected due to geometry of double horn ice, and it

can be inferred that the aerodynamic performance of NLF-0414 is very sensitive to double horn ice assertion.

(a)

(b)
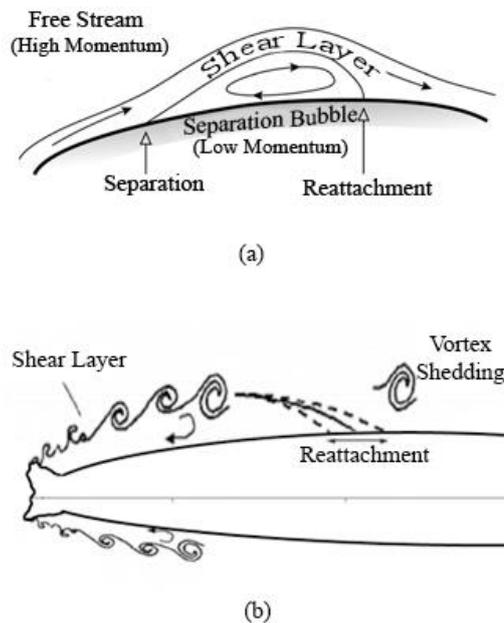
Fig.10. Qualitative sketch of formation and reattachment of shear layers (a) on a clean airfoil (b) downstream of horn-ice (Gurbacki 2003).

As shown in Figs. 5-6, for test cases of $\alpha = -2^{\circ}$ and $\alpha = 0^{\circ}$, pressure distribution over airfoil surface presents strange behavior (especially on the upper surface), which is very different to that for clean airfoil. The reason can be attributed to the unique geometry of double horn ice. When the airfoil heads straight into the wind, double horn ice at the leading edge acts more like a bluff body, and disarranges pressure distribution in a way which is not seen for the iced airfoil in higher angles of attack ($\alpha = 4^{\circ}$ and $\alpha = 6^{\circ}$).

4. CONCLUSION

This experimental research, investigates aerodynamic performance degradation of a NLF-0414 airfoil under a defined icing condition. Experiments are conducted for different angles of attack from -2 to 6 degrees. Shear layer reattachment locations are evaluated for upper and lower separation bubbles. The upper surface separation bubble increased in size and the lower surface separation bubble decreased in size as the angle of attack was increased. In all the experiments, pressure distribution on iced airfoil shows a large deviation from the clean airfoil, which is attributed to the large extent of separated flow.

REFERENCES

Barber, S., Y. Wang, S. Jafari, N. Chokani and R. S. Abhari (2011). The impact of ice formation on wind turbine performance and aerodynamics. *Journal of Solar Energy Engineering*133(1), 1-9.

Bose, N. (1992). Icing on a small horizontal-axis wind turbine—Part 1: Glaze ice profiles. *Journal of wind engineering and industrial aerodynamics*45(1), 75-85.

Bragg, M.B., A. Khodadoust and S.A. Spring (1992). Measurements in a leading-edge separation bubble due to a simulated airfoil ice accretion. *AIAA Journal*30(6), 1462-1467.

Bragg, M.B., A.P.Broeren and L.A.Blumenthal (2005). Iced-airfoil aerodynamics.*Progress in Aerospace Sciences* 41(5), 323-362.

Colin, S.B. (1991). Icing characteristics of a natural-laminar-flow, a medium-speed, anda swept, medium-speed airfoil. *29th Aerospace Sciences Meeting*, AIAA-91-0447, Reno, Nevada, USA,American Institute of Aeronautics and Astronautics.

Etemaddar, M., M.O.L. Hansen and T. Moan (2014). Wind turbine aerodynamic response under atmospheric icing conditions. *Wind Energy* 17(2), 241–265.

Fortin, G. and J. Perron (2009). Wind turbine icing and de-icing. *47th AIAA Aerospace Sciences Meeting and Exhibit*, AIAA-2009-274,Orlando, Florida, USA,American Institute of Aeronautics and Astronautics.

Fortin, G., J. Perron and A. Ilinca (2005). A study of icing events at Murdochville: conclusions for the wind power industry. *International Conference, Wind Energy in Remote Regions,* Magdalene Islands, Quebec, Canada.

Gurbacki, H.M (2003). *Ice-induced unsteady flowfield effects on airfoil performance*. Ph.D. Dissertation, Dept. of Aeronautical and Astronautical Engineering, University of Illinois, Urbana, USA.

Han, Y., J. Palacios and S. Schmitz (2012). Scaled ice accretion experiments on a rotating wind turbine blade. *Journal of Wind Engineering and Industrial Aerodynamics*109, 55-67.

Hochart, C., G. Fortin, J. Perron and A. Ilinca (2007). Icing Simulation of Wind Turbine Blades. *45th AIAA Aerospace Sciences Meeting and Exhibit*, AIAA-2007-1373, Reno, Nevada, USA,American Institute of Aeronautics and Astronautics.

Homola, M.C., M.S. Virk, P.J. Nicklasson and P.A. Sundsb (2012). Performance losses due to ice accretion for a 5 MW wind turbine. *Wind*

*Energy*15(3), 379-389.

Homola, M.C., T. Wallenius, L. Makkonen, P.J. Nicklasson andP.A. Sundsb (2010). Turbine size and temperature dependence of icing on wind turbine blades. *Wind Energy* 34(6),615–27.

Jin,Zh. Y., Q.T. Dong and Zh.G. Yang (2015). The effect of single-horn glaze ice on the vortex structures in the wake of a horizontal axis wind turbine. *Acta Mechanica Sinica*31(1), 62-72.

Katz, J. and A. Plotkin (2001).*Low Speed Aerodynamics from Wing Theory to Panel methods*, McGraw Hill.

Kim, H. and M. Bragg (1999). Effects of leading-edge ice accretion geometry on airfoil performance. *17th Applied Aerodynamics Conference*, American Institute of Aeronautics and Astronautics.

Lamraoui, F., G. Fortin, R. Benoit, J. Perron and C. Masson (2014). Atmospheric icing impact on wind turbine production. *Cold Regions Science and Technology*100, 36-49.

Lee, S. and M.B. Bragg (1999). Experimental Investigation of Simulated Large-Droplet Ice Shapes on Airfoil Aerodynamics.*Journal of Aircraft*36(5), 844-850.

Li Y., K. Tagawa andW. Liu (2010). Performance effects of attachment on blade on a straight-bladed vertical axis wind turbine. *Current Applied Physics* 10(2),S335-S338.

Li Y., Sh. Li andK. Tagawa (2011). Numerical simulation on icing effects on the pressure field around blade airfoil for straight-bladed VAWT. *International Journal of Agricultural and Biological Engineering*4(3),41–47.

Li, Y., K. Tagawa, F. Feng, Q. Li and Q. He (2014). A wind tunnel experimental study of icing on wind turbine blade airfoil. *Energy Conversion and Management*85, 591-595.

Li, Y., Y. Chi, F. Feng, K. Tagawa andW. Tian (2012). Wind tunnel test on blade surface icing for vertical axis wind turbine. *Journal of Engineering Thermophysics 33(11),1872–1875.*

Mirzaei, M., M.A. Ardekani and M. Doosttalab (2009). Numerical and experimental study of flow field characteristics of an iced airfoil. *Aerospace Science and Technology*13(6), 267-276.

Pryor, S.C. andR.J.Barthelmie (2010). Climate change impacts on wind energy: a review. *Renewable and Sustainable Energy Reviews* 14(1), 430-437.